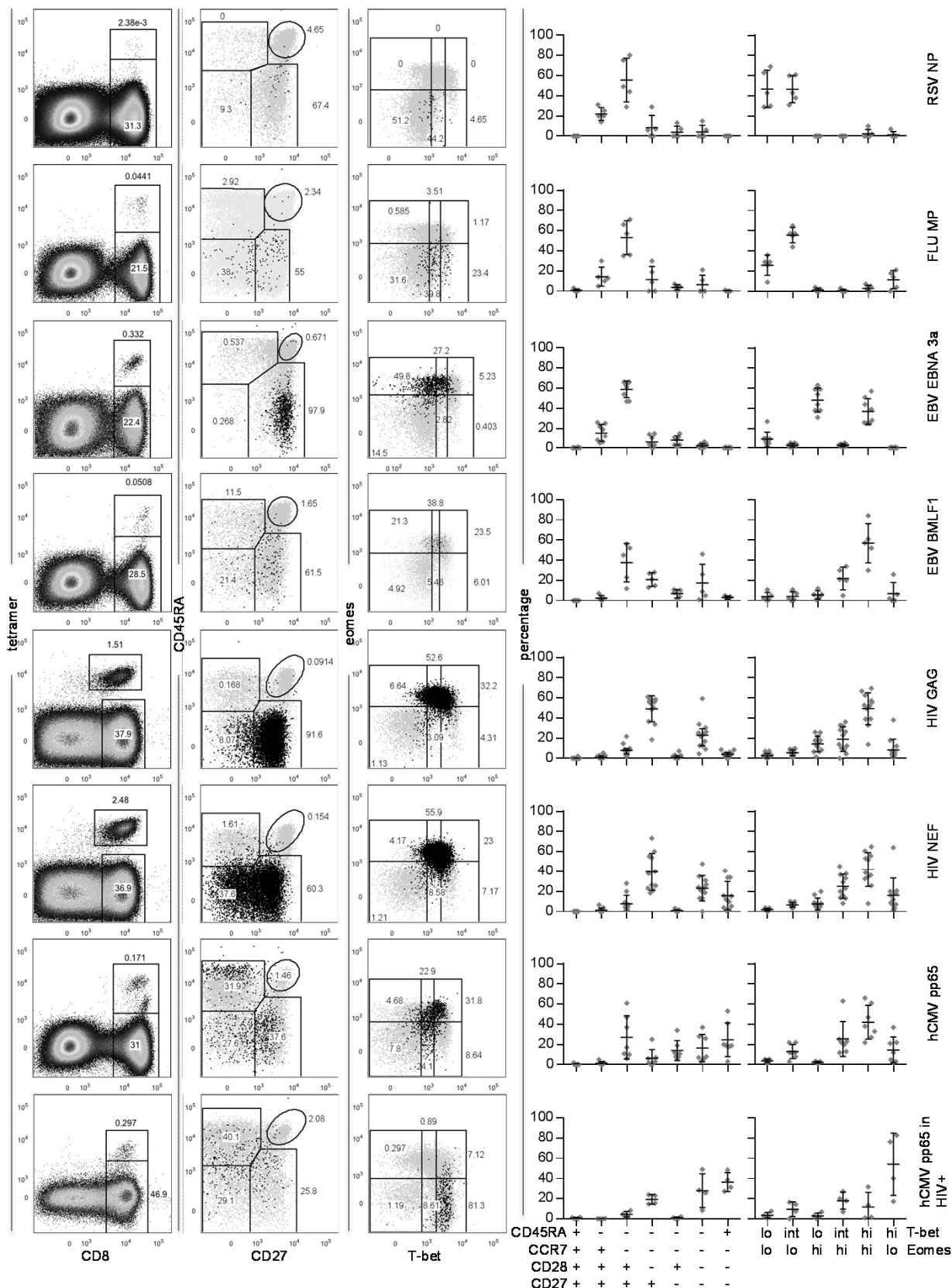
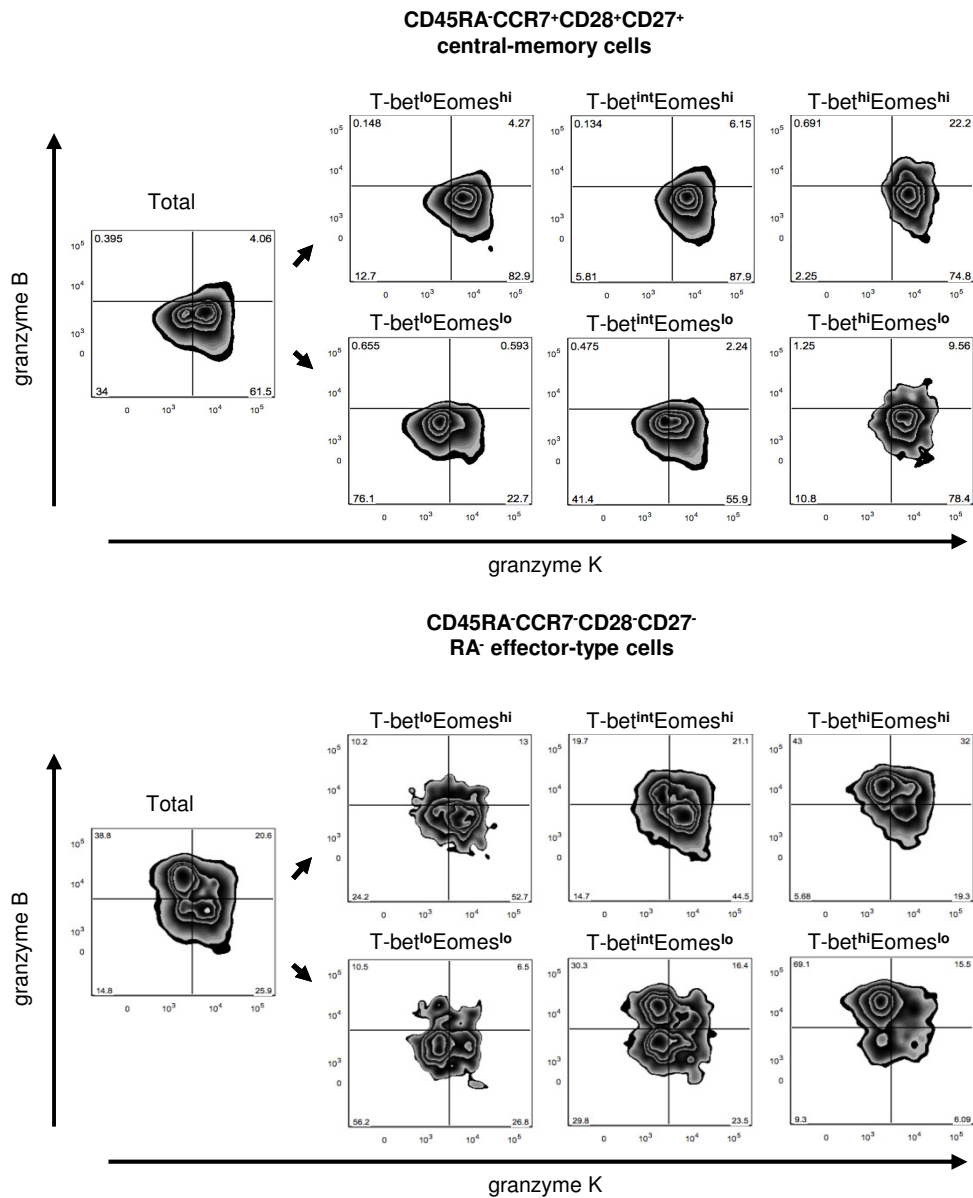


**Figure S1. Shifting associations between the surface phenotype and the T-bet/Eomes expression levels**  
**(a)** Representative dot plots showing the gating strategy used for defining the T-bet/Eomes gating populations, and **(b)** the gating strategy used for the other markers. Upper row from left to right: the lymphocyte gate (nb. after fixation and permeabilization), the sideward scatter width/height duplet exclusion, the forward scatter width/height duplet exclusion, the gating of CD3<sup>+</sup> tetramer<sup>+</sup> events, the gating of CD3<sup>+</sup>CD8<sup>+</sup>(tetramer<sup>+</sup>) events. Lower row from left to right: the gating of the CD45RA/CD27 CD8<sup>+</sup> T-cell populations, the gating of the CCR7-positive and negative CD8<sup>+</sup> T-cell populations, the gating of the CD28-positive and negative CD8<sup>+</sup> T-cell populations, and the expression frequencies of KLRG1, IL-7R $\alpha$ , granzyme K and granzyme B (lower row) **(c)** The distribution of the T-bet/Eomes expression states per CD45RA/CCR7/CD28/CD27-defined subset in 20 healthy- (left column) and 13 HIV-1-infected subjects (right column), mean/SD shown and **(d)**, reciprocally, the distribution of the CD45RA/CCR7/CD28/CD27-defined subsets over the T-bet/Eomes populations in 20 healthy- (left column) and 13 HIV-1-infected subjects (right column), mean/SD shown. The two HIV-1-infected patients not co-infected with hCMV are shown in red. See Figure 1 for statistical analyses.



**Figure S2. Virus-specific CD8<sup>+</sup> T-cells display distinct CD45RA/CCR7/CD28/CD27 and T-bet/Eomes expression levels**

Representative dot plots of the different virus-specific CD8<sup>+</sup> T-cell populations as stained with tetramers (left column), where CD8 fluorescence intensity (FI) is plotted on the X-axis and tetramer FI on the Y-axis, as well as their CD45RA (Y-axis)/CD27 (X-axis) and T-bet (X-axis)/Eomes (Y-axis) phenotypes presented as an overlay of the respective tetramer<sup>+</sup> population in black on the total CD8<sup>+</sup> T-cell population in gray. (Second column) The range of CD45RA/CCR7/CD28/CD27 phenotypes found among RSV NP- (n=5), influenza (Flu) MP1- (n=5), EBV EBNA-3a- (n=8), EBV BMLF-1- (n=5), HIV-1 gag- (n=12), HIV-1 nef- (n=11) and hCMV pp65-specific CD8<sup>+</sup> T-cells in healthy individuals (n=7) and in HIV-1-infected persons (n=4). (Middle column) The T-bet/Eomes expression states found among the same virus-specific populations, median and IQR shown. (Fourth and fifth columns) the surface marker- and T-bet/Eomes-defined subset distribution of hCMV pp65-specific cells circulating in healthy individuals (n=7) compared to the same populations in HIV-1-infected individuals (n=4), mean/SD shown. See Figure 2 for statistical analyses.



**Figure S3. An individual CD45RA/CCR7/CD28/CD27-defined subset comprises cells in different T-bet/Eomes expression states that are linked to functional differences**

Representative zebra plots of CD45RA<sup>+</sup> CCR7<sup>+</sup>CD28<sup>+</sup>CD27<sup>+</sup> central-memory cells (upper panel) and CD45RA<sup>-</sup> CCR7<sup>-</sup> CD28<sup>-</sup> CD27<sup>-</sup> effector-type cells (lower panel) plotting granzyme K fluorescence intensity on the X-axis and granzyme B fluorescence intensity on the Y-axis, and the shifts in the expression of these effector molecules per T-bet/Eomes expression state found in these CD45RA/CCR7/CD28/CD27-defined subsets.



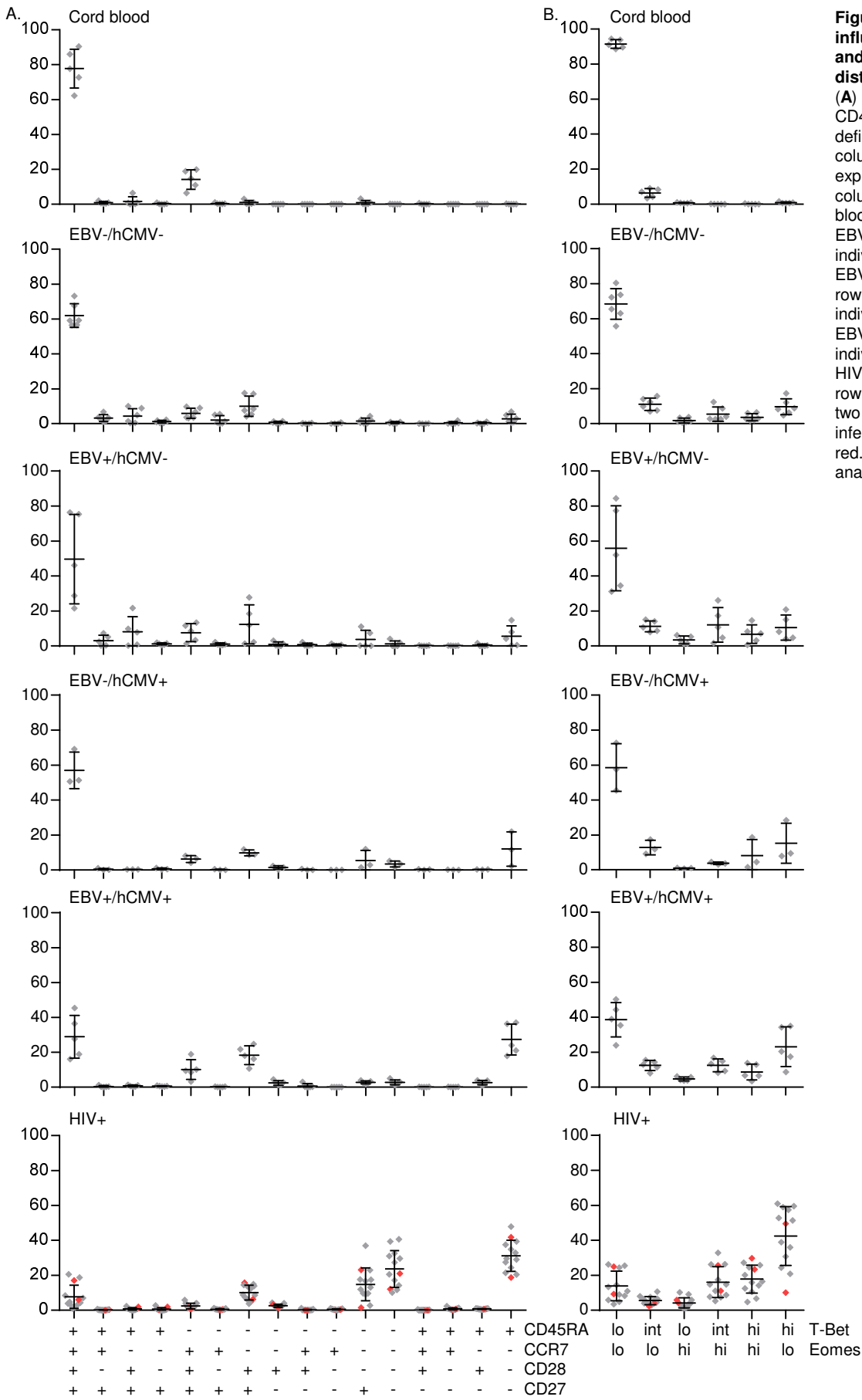


**Figure S5. Infection history influences the surface marker- and T-bet/Eomes-defined subset distribution**

(A) The CD45RA/CCR7/CD28/CD27-defined subset distribution (left column) and (B) the T-bet/Eomes expression state distribution (right column) over CD8<sup>+</sup> T-cells in cord blood samples (first row, n=5), EBV/hCMV seronegative individuals (second row, n=6), EBV seropositive individuals (third row, n=5), hCMV seropositive individuals (fourth row, n=3), EBV/hCMV double-infected individuals (fifth row, n=6) and HIV-1-infected individuals (last row, n=13), mean/SD shown. The two HIV-1-infected patients not co-infected with hCMV are shown in red. See Figure 5 for statistical analyses.



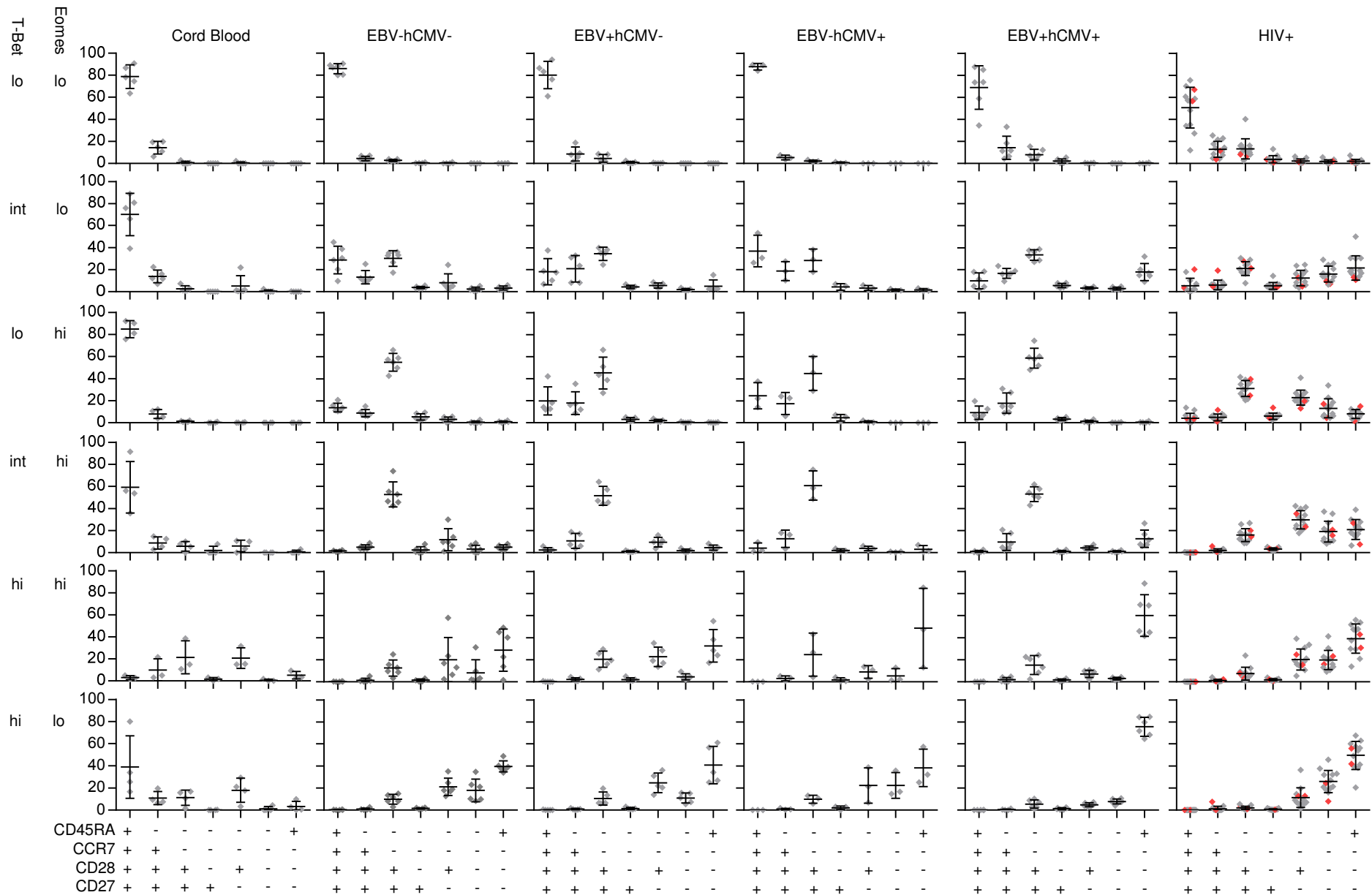


**Figure S6. Infection history influences the associations between T-bet/Eomes expression levels and surface phenotype**

Scatter plots displaying the relative distribution of the CD45RA/CCR7/CD28/CD27 phenotypes (plotted on the X-axis of each graph) over the different T-bet/Eomes expression states (rows) per study group: cord blood samples (first column, n=5), EBV/hCMV seronegative individuals (second column, n=6), EBV seropositive individuals (third column, n=5), hCMV seropositive individuals (fourth column, n=3), EBV/hCMV double-infected individuals (fifth column, n=6), and HIV-1-infected individuals (last column, n=13), mean/SD shown. The two HIV-1-infected patients not co-infected with hCMV are shown in red.

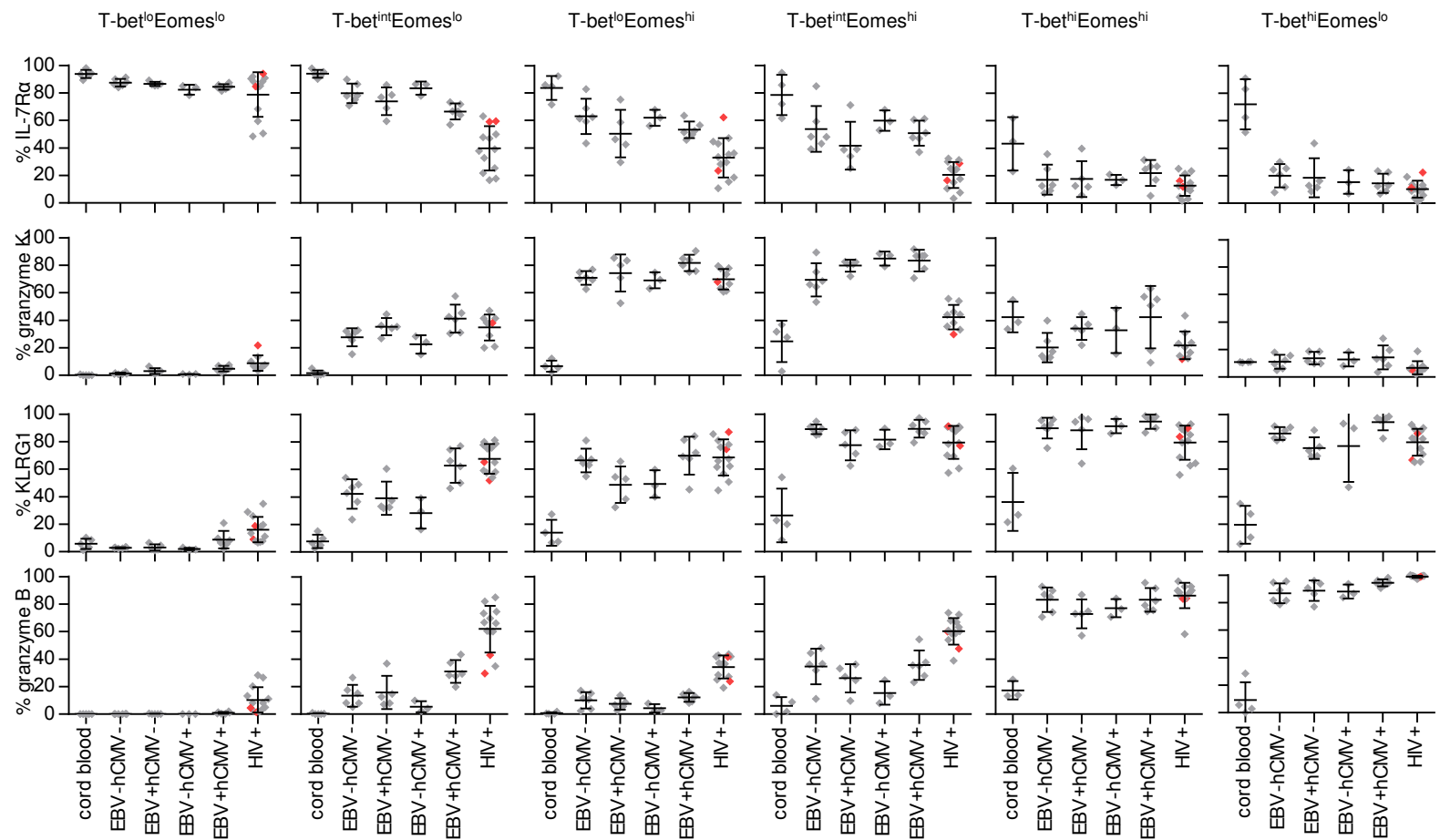


**Figure S7. Viral infection history impacts on the associations between the T-bet/Eomes expression levels and the functional potential**

Expression frequencies of IL-7R $\alpha$  (first row), granzyme K (second row), KLRG1 (third row) and granzyme B (last row) per T-bet<sup>lo</sup>Eomes<sup>lo</sup> (first column), T-bet<sup>int</sup>Eomes<sup>lo</sup> (second column), T-bet<sup>lo</sup>Eomes<sup>hi</sup> (third column), T-bet<sup>int</sup>Eomes<sup>hi</sup> (fourth column), T-bet<sup>hi</sup>Eomes<sup>hi</sup> (fifth column) and T-bet<sup>hi</sup>Eomes<sup>lo</sup> cells (last column) and per study group: cord blood samples, n=5; EBV/hCMV seronegative individuals, n=6; EBV seropositive individuals, n=5, hCMV seropositive individuals, n=3, EBV/hCMV double-infected individuals, n=6, and HIV-1-infected individuals (n=13) plotted on the X-axis of each graph, median and IQR shown. Note that not all cord blood samples comprised all T-bet/Eomes expression states. The two HIV-1-infected patients not co-infected with hCMV are shown in red.

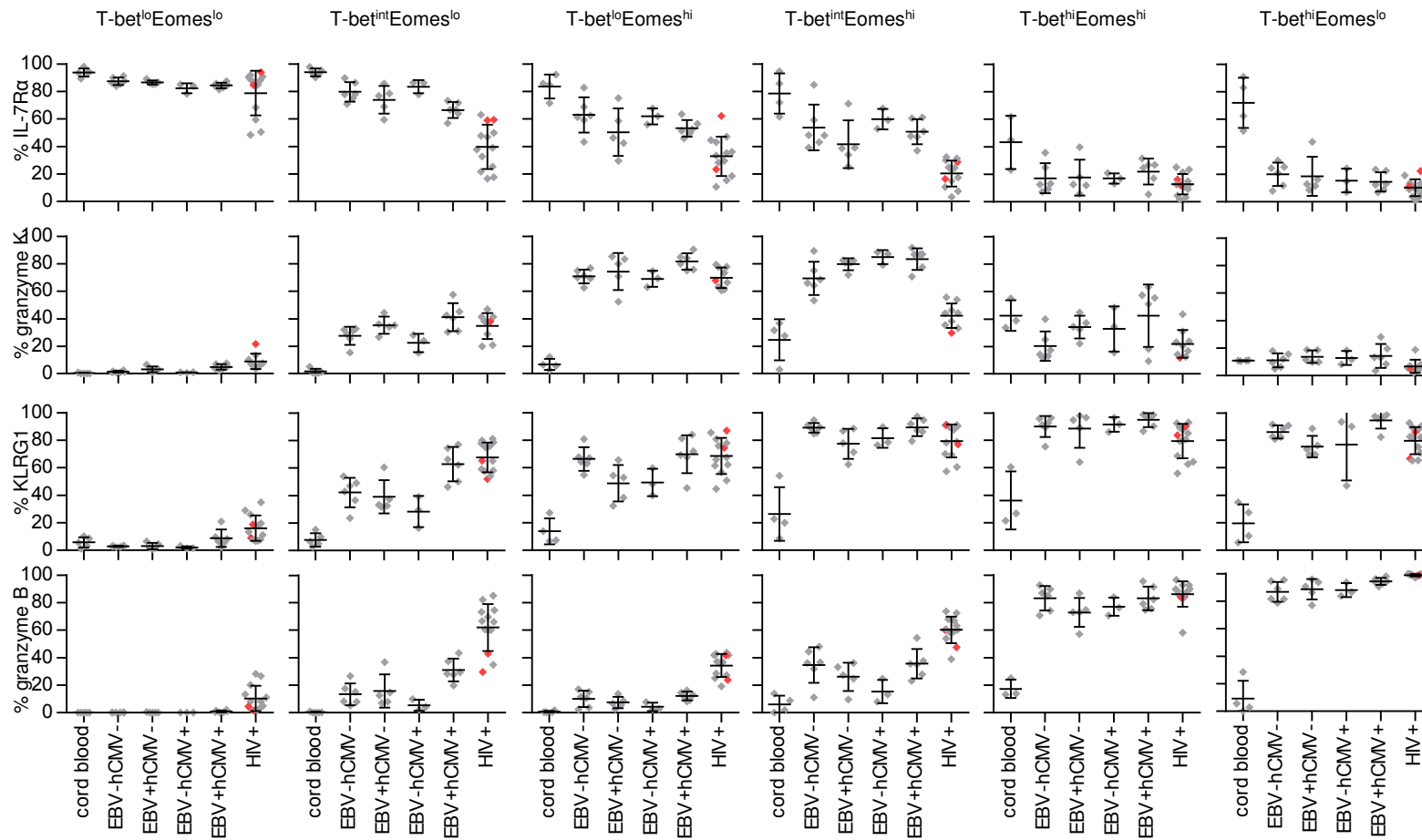


**Figure S8. Viral infection history impacts on the associations between CD45RA/CCR7/CD28/CD27 phenotype and the functional potential**

Expression frequencies of IL-7R $\alpha$  (first row), granzyme K (second row), KLRG1 (third row) and granzyme B (last row) per CD45RA/CCR7/CD28/CD27-defined subset (columns) and per study group: cord blood samples, n=5; EBV/hCMV seronegative individuals, n=6; EBV seropositive individuals, n=5, hCMV seropositive individuals, n=3, EBV/hCMV double-infected individuals, n=6 and HIV-1-infected individuals (n=13) plotted on the X-axis of each graph, mean/SD shown. Note that early-like and RA<sup>-</sup> effector-type populations were absent from cord blood, and that only two cord blood samples comprised sufficient RA<sup>+</sup> effector-type cells (>20 events) to be included in these analyses. The two HIV-1-infected patients not co-infected with hCMV are shown in red.



